Palaeogeography, Palaeoclimatology, Palaeoecology 371 (2013) 26–44

Contents lists available at SciVerse ScienceDirect

Palaeogeography, Palaeoclimatology, Palaeoecology

journal homepage: www.elsevier.com/locate/palaeo

Palaeoenvironmental and palaeoclimatic reconstruction of the Upper Cretaceous (late Campanian–early Maastrichtian) Horseshoe Canyon Formation, Alberta, Canada

Annie Quinney [a,*], François Therrien [a,b], Darla K. Zelenitsky [a], David A. Eberth [b]

[a] Department of Geoscience, University of Calgary, 2500 University Drive NW, Calgary, Alberta, Canada T2N 1N4
[b] Royal Tyrrell Museum of Palaeontology, P.O. Box 7500, Drumheller, Alberta, Canada T0J 0Y0

ARTICLE INFO

Article history:
Received 26 April 2012
Received in revised form 16 December 2012
Accepted 18 December 2012
Available online 5 January 2013

Keywords:
Paleosol
Palaeoenvironment
Palaeoclimate
Palaeopedology
Faunal change

ABSTRACT

Pedogenic features and geochemical signatures of paleosol profiles exposed in the Horseshoe Canyon Formation (HCFm) were studied to reconstruct the ancient environments and climates that prevailed at high latitude (~60°N) in the North American Western Interior during the late Campanian to early Maastrichtian. Eight pedotypes representing hydromorphic, moderately-drained and well-drained paleosols were recognized. When considered within their stratigraphic context, these paleosols show that palaeoenvironmental and palaeoclimatic changes occurred either gradually between major lithological subdivisions of the HCFm or relatively rapidly within subdivisions. Hydromorphic paleosols, predominant in the coal-bearing stratigraphic interval at the base of the HCFm, were gradually replaced by well-drained paleosols in the overlying coal-poor interval. While climate remained warm and humid during this change in soil drainage conditions, mean annual temperature and precipitation dropped rapidly higher in section, shortly prior to the Campanian–Maastrichtian boundary, without concomitant lithological or pedological changes. A brief return of poorly-drained paleosols in the middle of the HCFm coincides with a regional marine transgression (Drumheller Marine Tongue). Well-drained palaeoenvironments, associated with a warm and dry climate, persisted through the upper part of the HCFm until a gradual return to poorly-drained conditions and to a warm, humid climate occurred at the top of the formation. An important decline in turtle diversity through the HCFm, previously attributed to climate, is shown to coincide instead with changes in soil drainage conditions, where aridity, landscape instability, and migratory barriers possibly acted as secondary limiting factors to faunal recovery.

1. Introduction

The Upper Cretaceous Horseshoe Canyon Formation (HCFm) is renowned for preserving one of the best high-latitude vertebrate fossil records in North America (e.g., Eberth et al., 2001; Brinkman and Eberth, 2006; Wu et al., 2007; Eberth and Currie, 2010; Larson et al., 2010). As such, it has been the subject of numerous studies that aimed at documenting the palaeoenvironmental and palaeoclimatic conditions and the biotic turnovers that characterized the end of the Cretaceous (e.g., Srivastava, 1970; Wolfe and Upchurch, 1987; McCabe et al., 1989; Brinkman, 2003; Hamblin, 2004; Lerbekmo and Braman, 2005; Brinkman and Eberth, 2006; Eberth and Braman, 2012). While these studies have recognized broad environmental and climatic trends and inferred a link between a dramatic decline in turtle diversity and palaeoclimate through the HCFm, few have sought to determine palaeoenvironmental parameters (e.g., palaeotemperature, palaeoprecipitation) or the precise stratigraphic position of palaeoenvironmental changes.

In this study, the palaeoclimatic and palaeoenvironmental conditions of the HCFm are reconstructed based on paleosols present in the formation. Detailed study of the pedogenic features and geochemical composition of HCFm paleosols provides valuable information on palaeoenvironmental parameters that could not be evaluated by previous studies. Furthermore, consideration of each paleosol in its stratigraphic context provides a detailed record of palaeoenvironmental and palaeoclimatic changes through the formation. This study aims to determine: 1) the palaeoenvironmental conditions that prevailed during deposition of the HCFm, 2) if lithological features (e.g., presence/absence of coal) are adequate palaeoenvironmental and palaeoclimatic indicators in the HCFm, and 3) if changes in turtle diversity through the HCFm can be better explained by factors other than climate.

2. Geologic setting

The depositional history of the HCFm has been influenced by tectonic activity, relative sea level change, and climate change (see Eberth and Braman, 2012 for a review). Deposited in southern Alberta in the Western Canada Sedimentary Basin, the HCFm comprises the basal two-thirds of an eastward thinning, clastic wedge of marginal marine to non-marine sediments known as the Edmonton Group.

* Corresponding author at: School of Geosciences, Monash University, Clayton campus, Wellington Road Clayton, Victoria 3800, Australia. Tel.: +1 468 784 353.
E-mail address: aequinne@gmail.com (A. Quinney).

0031-0182/$ – see front matter © 2012 Elsevier B.V. All rights reserved.
http://dx.doi.org/10.1016/j.palaeo.2012.12.009

Sediments of the Edmonton Group are terrestrially-derived from the concurrently-forming Rocky Mountains to the west, with the accretion of terranes preceding sedimentation into the basin (Cant and Stockmal, 1989; Catuneanu et al., 2000). Specifically, deposition of the HCFm is synchronous, in part, with the accretion of the Pacific Rim–Chugach Terrane during the Maastrichtian (Cant and Stockmal, 1989). A complex interplay of orogenic pulses and quiescent phases resulted in the respective creation and reduction of accommodation space throughout the deposition of the HCFm (Catuneanu et al., 2000; Eberth and Braman, 2012).

The HCFm was deposited during the late Campanian and early Maastrichtian (74–67 Ma) (Lerbekmo and Braman, 2002; Eberth and Braman, 2012) on the western shore of the Bearpaw Sea at a palaeolatitude of ~60°N (Smith et al., 1981; Larson et al., 2010). The Bearpaw Sea, defined as the entire 3rd order transgressive–regressive cycle of the Bearpaw cyclothem (sensu Catuneanu et al., 2000), was an extensive, northwest–southeast trending epeiric seaway that developed between the Canadian Shield to the east and the actively-forming Rocky Mountains to the west (Stott, 1984). During the late Campanian, the Bearpaw Sea gradually withdrew and the paralic to alluvial sediments of the HCFm prograded to the south and east. The contact between the Horseshoe Canyon Formation and the underlying marine Bearpaw Formation is conformable and records the overall and final regression of the Bearpaw Sea (Leckie and Smith, 1992; Hamblin, 2004; Eberth and Braman, 2012).

In the Drumheller area, exposures of the HCFm are approximately 250 m thick (composite section) and consist of interbedded sandstones, siltstones, shales, and coals that were generally deposited by high-sinuosity fluvial systems in coastal to alluvial settings (Hamblin, 2004; Eberth and Braman, 2012). Thirteen coal seams or swarms (i.e., associated coal beds occurring in close stratigraphic proximity, see Straight and Eberth, 2002) are recognized and numbered consecutively from 0 to 12 (Gibson, 1977). Eberth (2004) subdivided the HCFm into five informal units based upon lithological differences observable in outcrops, inferred to reflect eustatic, tectonic, and/or climatic controls. The basal unit of the HCFm (Unit 1) is approximately 150–160 m thick and consists of brown, gray, and green mudstones interbedded with siderite layers and laterally extensive carbonaceous mudstones and sandstones. At least 10 laterally-extensive coal intervals (coals 0–9) have been recorded within this unit (Gibson, 1977; McCabe et al., 1989). Unit 1 is overlain by the 30 m-thick Unit 2, which consists of olive green to gray-green mudstones interbedded with laterally-extensive sandstones. A stratigraphic

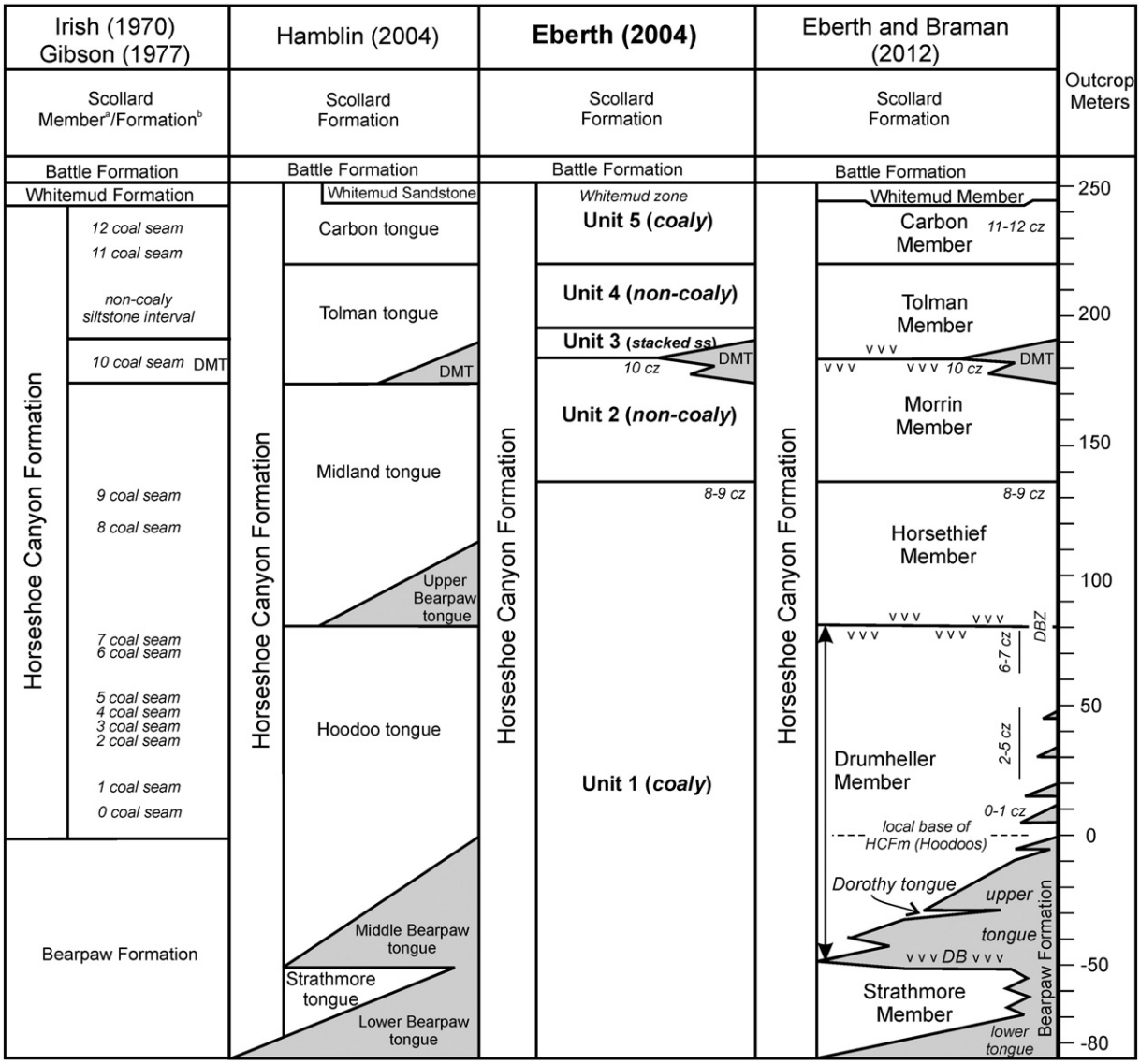

Fig. 1. Comparison of intraformational stratigraphic schemes for the Horseshoe Canyon Formation. Abbreviations: cz, Coal Zone; DB, Dorothy Bentonite; DBZ, Drumheller Bentonite Zone; DMT, Drumheller Marine Tongue; ss, sandstone; vvv, stratigraphic interval rich in bentonite. Data from Irish (1970).

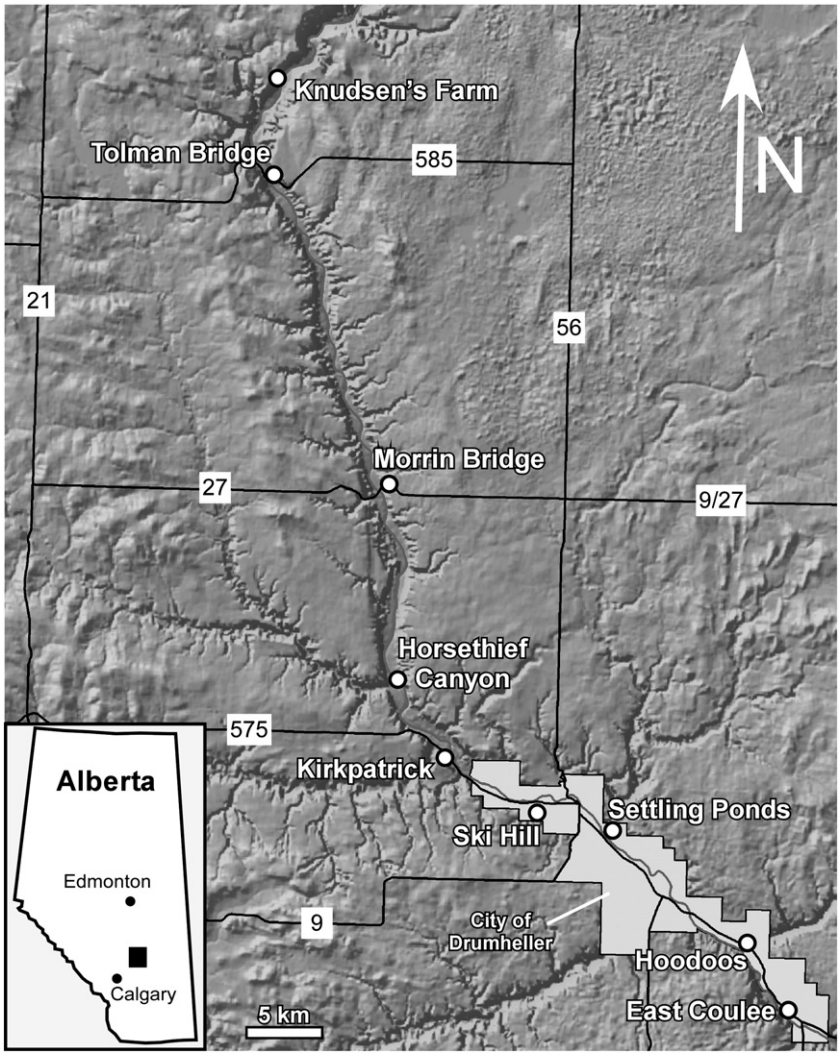

Fig. 2. Location of eight stratigraphic sections considered in this study. The Knudsen's Farm locality was investigated by Forkner (2002) and integrated in this study. Inset illustrates location of study area (black square) in south-central Alberta.

interval of variable thickness, containing a single coal bed (Coal 10) and numerous occurrences of brackish-water pelecypods, occurs in the middle of Unit 2 and is associated with a significant marine transgression referred to as the "Drumheller Marine Tongue." Unit 3 is a 10–20 m-thick non-coaly interval that consists predominantly of laterally extensive, light brown, fine-grained, stacked sandstones and rare fine-grained deposits. Unit 4, approximately 25 m thick, is a non-coaly interval that consists of light green to green-gray mudstones and fine-grained, single-storied sandstones represented in subequal proportions. Finally Unit 5, the uppermost unit of the HCFm, is approximately 20 m thick and consists of light gray mudstones interbedded with laterally-extensive sandstone bodies and two coal swarms (Coal 11 and 12; Hamblin, 2004; Eberth, 2004). Although some researchers have recently included the Whitemud Formation as a subunit of the HCFm (Hamblin, 2004; Eberth and Braman, 2012), this unit was not investigated in the context of the current project.

Alternative intra-formational stratigraphic schemes have been proposed for the HCFm, but we employ that of Eberth (2004) because it was the most widely used at the time of this study (e.g., Wu et al., 2007; Larson et al., 2010; Mallon et al., 2011). For the reader's benefit, we present a correlation chart (Fig. 1) that compares the stratigraphic scheme of Eberth (2004) to those of other authors, including the recently published scheme of Eberth and Braman (2012). With two minor exceptions, the boundaries of units 1–5 of Eberth (2004) correspond to boundaries of the formal members described by Eberth and Braman (2012). Consequently, the results of our study apply equally well in the context of this most recent stratigraphic scheme.

3. Methods

During the summer of 2010, paleosols were documented at six stratigraphic sections previously measured by Eberth and Braman (2012) and at two sections more recently measured by Quinney (2011). All measured sections are located within the Red Deer River Valley of south-central Alberta (Fig. 2) and, once correlated, span the entire stratigraphic interval of the HCFm (Fig. 3). Paleosol profiles were identified based on the presence of pedogenic horizons, root traces, and macroscopic pedogenic features. Each paleosol was

Fig. 3. Correlated sections showing the stratigraphic distribution of pedotypes within the Horseshoe Canyon Formation. Numbers appearing next to sections represent paleosol categories. Dash lines represent marker beds used to correlate stratigraphic sections. Italicized numbers represent named coal beds. Alternating white and gray stratigraphic intervals represent HCFm subdivisions of Eberth (2004). Each stratigraphic interval is represented by at least two measured sections, except for Unit 3. Hollow box in Units 2 and 3 represents stratigraphic interval known as the Drumheller Marine Tongue. Knudsen's Farm section is modified from Forkner (2002). Black units are coal beds. Asterisks denote paleosol profiles selected as pedotypes.

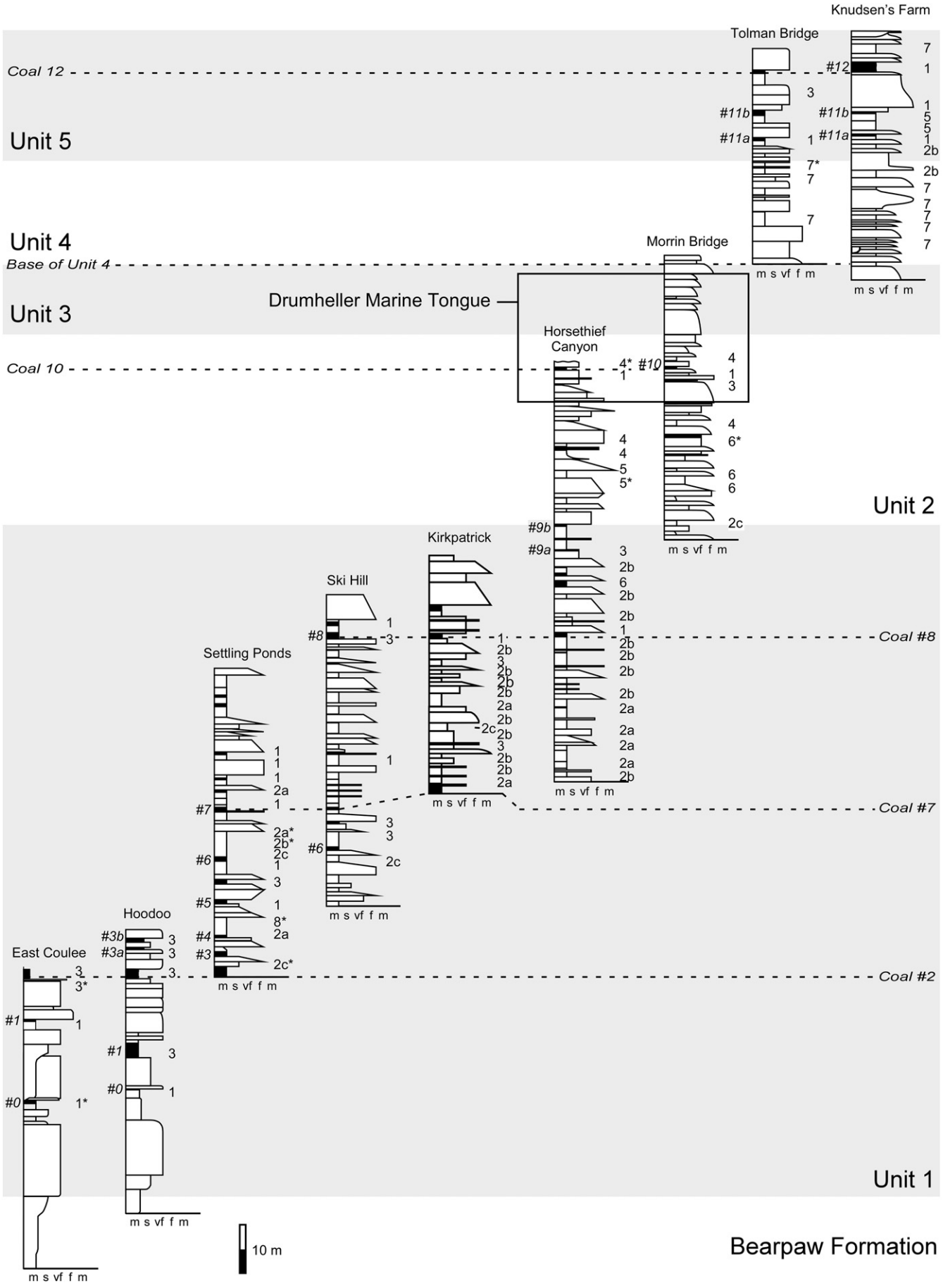
Knudsen's Farm
Tolman Bridge
Coal 12
Unit 5
Unit 4
Base of Unit 4
Unit 3
Drumheller Marine Tongue
Morrin Bridge
Horsethief Canyon
Coal 10
Unit 2
Kirkpatrick
Ski Hill
Settling Ponds
Hoodoo
East Coulee
Coal #8
Coal #7
Coal #2
Unit 1
m s vf f m
10 m
Bearpaw Formation

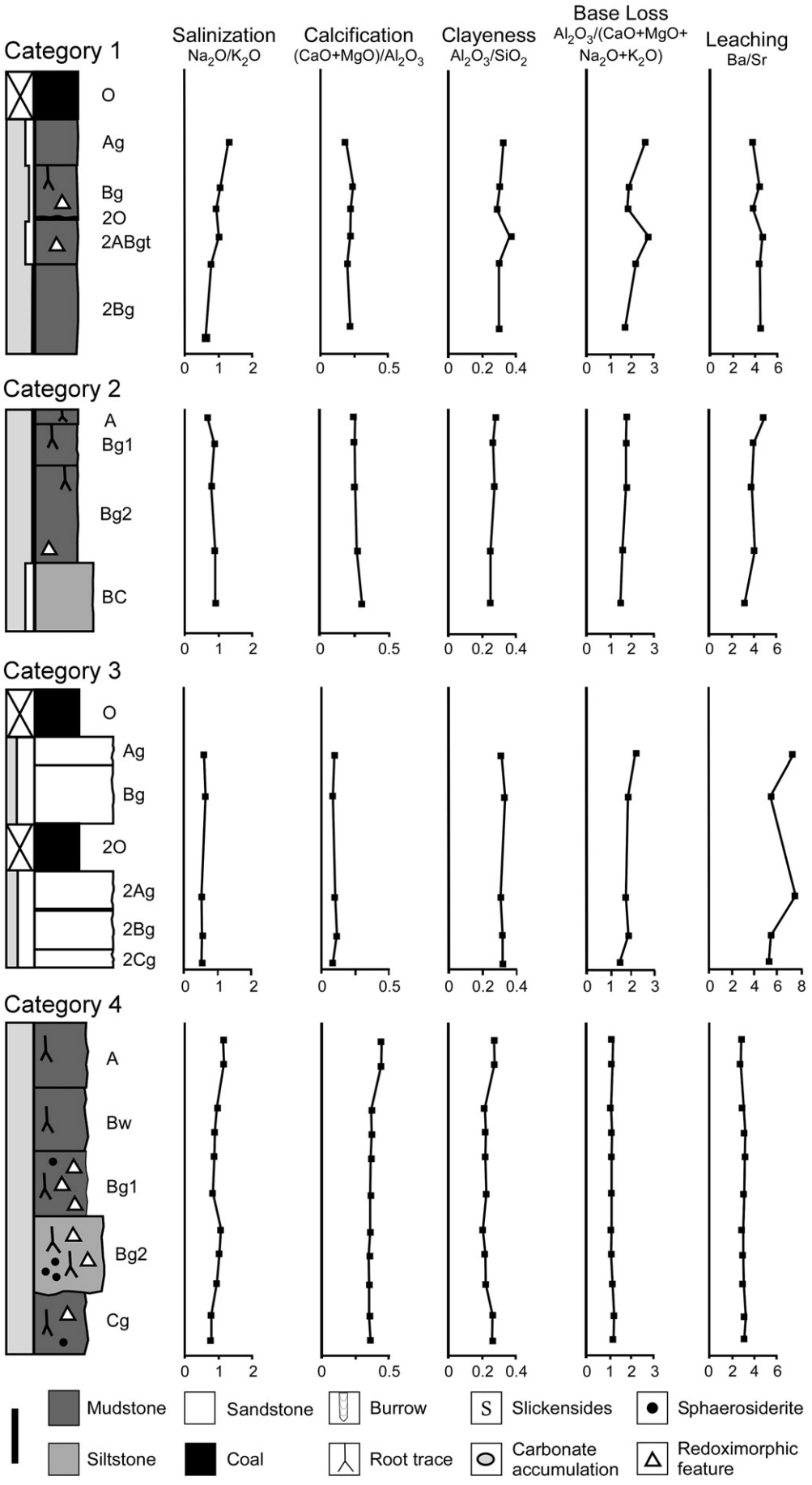
Salinization
Na_2O/K_2O
Calcification
$(CaO+MgO)/Al_2O_3$
Clayeness
Al_2O_3/SiO_2
Base Loss
$Al_2O_3/(CaO+MgO+Na_2O+K_2O)$
Leaching
Ba/Sr
Category 1
O
Ag
Bg
2O
2ABgt
2Bg
Category 2
A
Bg1
Bg2
BC
Category 3
O
Ag
Bg
2O
2Ag
2Bg
2Cg
Category 4
A
Bw
Bg1
Bg2
Cg
Mudstone
Siltstone
Sandstone
Coal
Burrow
Root trace
S
Slickensides
Carbonate accumulation
Sphaerosiderite
Redoximorphic feature

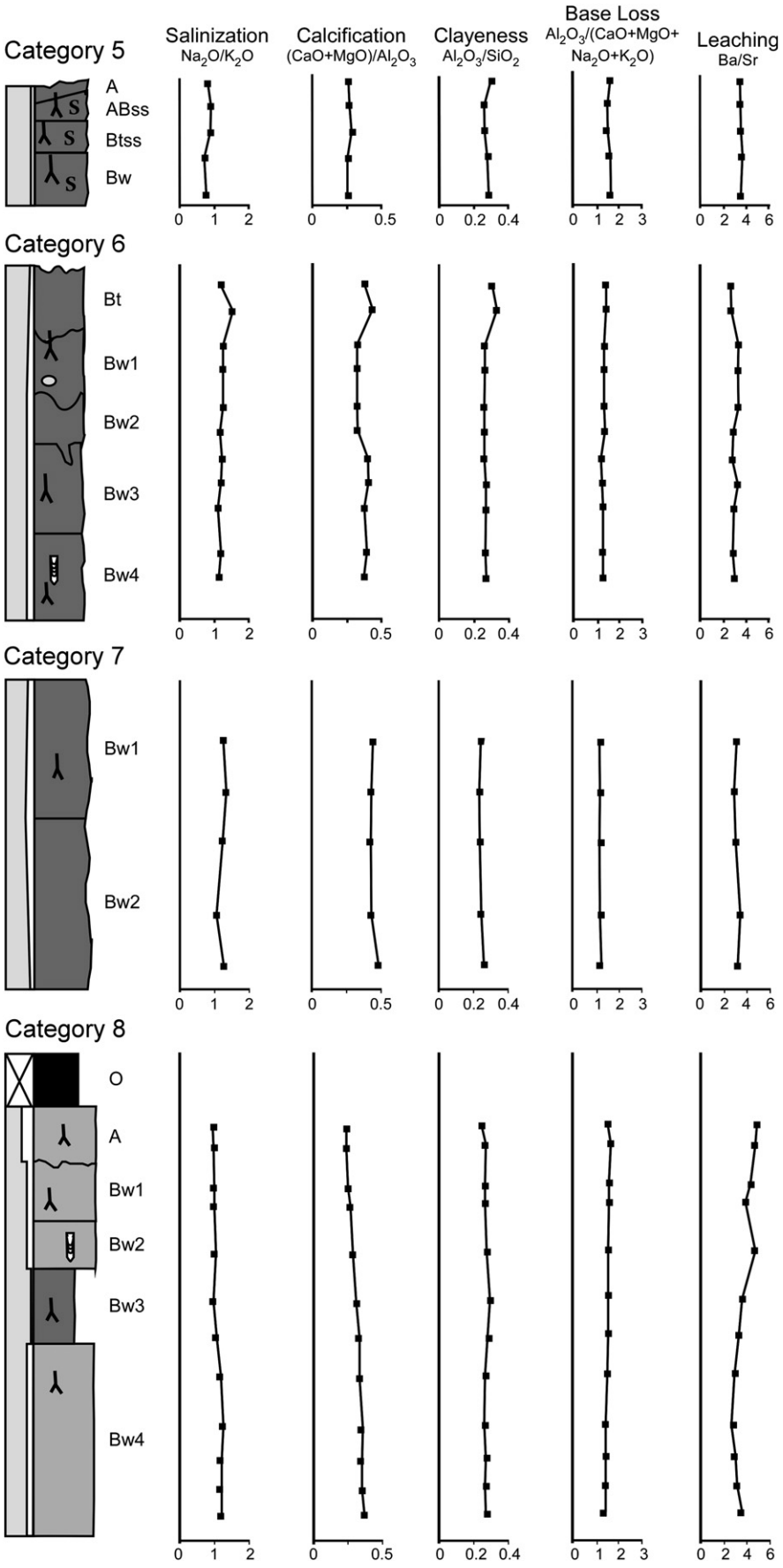

Fig. 4. Pedotypes for eight paleosol categories recognized in the Horseshoe Canyon Formation. The textural indicator (column to the left of the stratigraphic section) reflects the proportion of fine (clay + silt in gray) to coarse (sand in white) grains throughout the profile determined by point counting. Scale bar equals 30 cm.

documented in the field in terms of horizon thickness, color, lithology, macroscopic pedogenic features, sedimentary structures, and stratigraphic position within the HCFm. Where possible, paleosols were exposed laterally in order to document lateral variation. Thickness measurements were made using a tape measure and horizon color was documented using the Munsell Soil Colour chart (Munsell, 2005). Due to the microscopic nature of the redoximorphic features, the color of these features could not be evaluated.

Fresh rock samples were collected at a 15–20 cm interval in each paleosol profile for petrographic and geochemical study. Ninety-eight thin sections were prepared from these samples and paleosol micromorphology was described following the terminology of Bullock et al. (1985). Relative abundance of sand versus mud and silt in pedogenic horizons was evaluated through point counting. Bulk geochemistry was determined for 152 samples through X-ray fluorescence spectroscopy (XRF). These results were used to calculate molecular weathering ratios, which are used as a geochemical proxy for pedogenic processes (Feakes and Retallack, 1988; Retallack, 1997), and to calculate mean annual precipitation (MAP) and mean annual temperature (MAT) estimates (Sheldon et al., 2002; Sheldon, 2006; Sheldon and Tabor, 2009; Nordt and Driese, 2012). Due to the uncertainty surrounding the geochemical composition of the parent material(s) of HCFm paleosols, the mass-balance method for paleosol geochemical analysis (e.g., Chadwick et al., 1990; Driese et al., 2000) was not utilized.

Paleosols of the HCFm are classified into pedotypes, inferred to represent paleosol profiles that formed under a similar set of palaeoenvironmental and palaeoclimatic conditions (Retallack, 1994), based on macroscopic and microscopic pedogenic features and molecular weathering ratios. Pedotypes are assigned to a paleosol order following the classification of Mack et al. (1993). Palaeoenvironmental and palaeoclimatic reconstructions are based solely on the pedogenic features and geochemical indicators of each paleosol profile, without reference to modern soil taxonomy, in order to avoid interpretation biases (see Fastovsky and McSweeney, 1987; Mack et al., 1993; Dahms, 1998; Dahms and Holiday, 1998). Palaeoenvironmental and palaeoclimatic indicators were considered in the stratigraphic context of each paleosol profile within the HCFm. Results of the present study are complemented by Forkner's (2002) study of paleosols of the upper HCFm (Units 4 and 5) exposed at Knudsen's Farm (Fig. 2). The Knudsen's Farm section was briefly visited to integrate Forkner's (2002) pedotypes into the present study.

The effects of diagenesis on HCFm paleosol geochemistry and pedogenic features are considered minor due to the absence of observable diagenetic features, such as recrystallization or burial reddening (e.g. Fastovsky and McSweeney, 1987; Retallack, 1997). Furthermore, the estimated depth of burial of the HCFm is very shallow (less than 2 km: Nurkowski, 1984; Khidir and Catuneanu, 2009), suggesting that diagenetic changes would have been limited. Consequently, the pedogenic features and geochemical composition of HCFm paleosols are considered to represent the original signature of Upper Cretaceous palaeoenvironmental and palaeoclimatic conditions.

4. Results

Seventy-nine paleosol profiles, varying in thickness between 45 and 185 cm, were identified in the HCFm (Fig. 3) and classified into eight pedotypes (Fig. 4, Table 1). Individual profiles tend to fine upwards and can either be separated vertically by sandstone sheets or stacked, forming compound or composite profiles (e.g. Kraus and Brown, 1986; Kraus, 1999). Truncated paleosol profiles with erosional upper contacts were also observed, most commonly in Units 2 and 4. Although most paleosol profiles are laterally extensive, some profiles developed in lenticular channel fill deposits and are restricted to approximately 20 m in lateral extent.

4.1. Category 1 paleosols: low-chroma profile capped by coal horizon

This pedotype is common in the HCFm and represents 20.5% of the paleosols encountered (n = 16). Category 1 paleosols consist of low-chroma (chroma = 1) brown, gray, or green-gray profiles overlain by a coal horizon varying between 15 and 120 cm thick (Figs. 4 and 5a, Table 1). Although carbonaceous root fossils are the only macroscopic pedogenic feature observable, study of thin sections reveals that clay coatings and redoximorphic features (ferruginous hypocoatings) decrease and increase, respectively, in abundance upward through the profile. Geochemically, these paleosols show limited changes in molecular weathering ratios through the profile (Fig. 4).

4.2. Category 2 paleosols: low-chroma profiles with a thin, organic-rich surficial horizon

This pedotype is extremely common in the HCFm, representing 39% of the paleosols encountered (n = 31). Category 2 paleosols consist of low-chroma mudstone to siltstone horizons overlain by an organic-rich mudstone (Fig. 4, Table 1). Although the predominant color of the subsurface horizons varies from gray to green to brown (Category 2a, 2b, and 2c, respectively), all Category 2 paleosols display similar pedogenic features (see Table 1). Slickensides, redoximorphic features (ferruginous masses and hypocoatings), limited clay accumulation, and carbonaceous root fossils are observable in thin sections (Fig. 6A–C). Category 2 paleosols show limited geochemical differentiation between horizons (Fig. 4).

4.3. Category 3 paleosols: pedogenically-modified sandstone overlain by coal horizon

This pedotype is common in the HCFm, representing 19% of paleosols (n = 15). Category 3 paleosols consist of low-chroma, white to green-gray, fine- to medium-grained sandstones capped by a thick (30–200 cm) coal horizon (Fig. 4, Table 1). The sandstone horizons exhibit relict sedimentary structures, abundant and well-developed clay coatings, and common ferruginous hypocoatings. The horizons of Category 3 paleosols are geochemically undifferentiated, except for the leaching and base loss ratios, which decrease with depth (Fig. 4). Furthermore, the leaching ratio reaches the highest values observed in any of the HCFm pedotypes.

4.4. Category 4 paleosols: profiles with low-chroma basal horizons and higher-chroma upper horizons

This pedotype is uncommon in the HCFm, representing 6.5% of the paleosols (n = 5). Category 4 paleosols consist of low-chroma (chroma = 1), gray to green-gray mudstone horizons in the lower part of the profile and of higher-chroma (chroma = 2), olive-colored mudstone horizons in the upper part (Figs. 4 and 5b, Table 1). Clay coatings and redoximorphic features (ferruginous masses) decrease in abundance upward through the profile. Sphaerosiderite nodules are present in these paleosols (Fig. 6D), occurring as small (5–20 μm in diameter), grape-like clusters in the groundmass, with the largest (up to 30 μm in diameter) and most abundant nodules occurring low in the paleosol profile. Geochemical differentiation of horizons is limited in the lower part of the profile, but an increase in the salinization, clayeness and calcification ratios is observed near the top of the profile (Fig. 4). Notably, the calcification and leaching ratios are higher and lower, respectively, than in Category 1–3 paleosols.

4.5. Category 5 paleosols: varicolored profiles with slickensides

This pedotype is rare in the HCFm, representing 5% of the paleosols (n = 4). Category 5 paleosols consist of a succession of thin (9–32 cm), higher-chroma, varicolored horizons (Fig. 4, Table 1), although a thick (~50 cm), low-chroma horizon is present at the base of one profile

Table 1
Characteristics of Horseshoe Canyon Formation pedotypes.

Category 1: pedotype 102 m above base of HCFm; 45.5 m above base of Settling Ponds section; 73–123 cm thick; mean thickness 71 cm

Mack et al.'s (1993) paleosol type: gleyed histosol

Depth (cm)	Horizon	Lithology	Color	B-fabric and Microscopic Pedofeatures	Redoximorphic features	Notes
0–27	O	Coal	Black	None observed	None observed	
27–44	Ag	Mudstone	Dark gray (10YR 4/1)	Stipple-speckled b-fabric Uncommon clay coatings	None observed	
44–73	Bg	Mudstone	White (5Y 8/1)	Stipple-speckled to mosaic-speckled b-fabric Common clay coatings	Uncommon ferruginous hypocoating around root fossil; weak iron accumulation in groundmass	Carbonaceous root fossil
73–76	2O	Coal	Black	None observed	None observed	
76–109	2ABg	Mudstone	Light gray (10YR 7/1)	Stipple-speckled to unistriated b-fabric Common, well-developed clay coatings	Rare ferruginous hypocoating along root trace	Root trace
109–196	2Bg	Mudstone	Gray (10YR 6/1)	Very well developed mosaic-speckled b-fabric Common, well-developed clay coatings	None observed	

Category 2a: pedotype 76 m above base of HCFm; 28.5 m above base of Settling Ponds section; 83–130 cm thick, mean thickness 109.9 cm

Mack et al.'s (1993) paleosol type: gleysol

Depth (cm)	Horizon	Lithology	Color	B-fabric and Illuvial features	Redoximorphic features	Notes
0–15	Ag	Organic-rich mudstone	Grayish brown (10YR 5/2)	Mosaic-speckled to unistriated b-fabric Common, weakly developed clay coatings	None observed	Root traces, Carbonaceous root fossils, Possible slickensides
15–41	Bg1	Mudstone	Light gray (5Y 7/1)	Unistriated to mosaic-speckled b-fabric Common moderately developed clay coatings	None observed	Possible slickensides
41–63	Bg2	Mudstone	Light gray (5Y 7/1)	Unistriated to stipple-speckled b-fabric Common moderately developed clay coatings	None observed	Burrow, Possible slickensides
63–76	BC	Mudstone	Light brownish gray (2.5Y 6/2)	Stipple-speckled to mosaic speckled b-fabric Uncommon, weakly developed clay coatings	None observed	Burrow/root trace

Category 2b: pedotype 70 m above base of HCFm; 26.5 m above base of Settling Ponds Section; 40–244 cm thick; mean thickness 132.1 cm

Mack et al.'s (1993) paleosol type: gleysol

Depth (cm)	Horizon	Lithology	Color	B-fabric and Illuvial features	Redoximorphic Features	Notes
0–5	A	Mudstone	Very dark gray (2.5Y 3/1)	Well-developed reticulate b-fabric (Slickensides)		Possible root trace/burrows
5–21	Bg1	Mudstone	Greenish gray (10GY 5/1)	Well-developed unistriated to reticulate b-fabrics (Slickensides)		Root trace
21–67	Bg2	Mudstone	Dark greenish gray (5GY 4/1)	Well-developed reticulate to stipple-speckled b-fabric Uncommon, weakly-developed clay coatings	Uncommon ferruginous hypocoating along carbonaceous root fossil and ped? surfaces	Root traces, Carbonaceous root fossils
67–90	BC	Siltstone	Greenish gray (10GY 5/1)	Well-developed mosaic-speckled b-fabric Rare granostriation Uncommon, moderately developed clay coatings		

(continued on next page)

Table 1 (*continued*)

Category 2c: pedotype 48 m above base of HCFm; 2 m above base of Settling Ponds Section; 31–156 cm thick; mean thickness 106.3 cm

Mack et al.'s (1993) soil type: gleysol

Depth (cm)	Horizon	Lithology	Color	B-fabric and Illuvial features	Redoximorphic Features	Notes
0–16	ABg	Mudstone	Dark grayish brown (10YR 4/2)	Mosaic speckled to unistriated b-fabric Uncommon, weakly developed clay coatings	Rare, weakly developed, ferruginous redoximorphic features (masses)	
16–23	Bg	Claystone	Grayish brown (10YR 5/2)	Stipple-speckled to mosaic speckled b-fabric Rare granostriation	Rare, weakly developed, ferruginous redoximorphic features (masses)	Root traces
23–31	CBg	Claystone	Dark grayish brown (10YR 4/2)	Unistriated b-fabric Rare granostriation	Rare, weakly developed, ferruginous redoximorphic features (masses)	

Category 3: pedotype 45 m above base of HCFm; 60 m above base of East Coulee section; 30–244 cm thick; mean thickness 91.7 cm

Mack et al.'s (1993) paleosol type: gleyed protosol

Depth (cm)	Horizon	Lithology	Color	B-fabric and Illuvial features	Redoximorphic features	Notes
0–21	O	Coal	Black	None observed	None observed	
21–37	Ag	Sandstone	White (10YR 8/1)	Stipple-speckled b-fabric Common granostriation Very common, well-developed clay coatings Very common iron coatings on grains, sometimes forming bridges/pendants and link cappings	None observed	
37–53	Bg	Sandstone	White (5Y 8/1)	Unistriated to mosaic-speckled b-fabric Common granostriation Very common, well-developed clay coatings Common iron coatings on grains, sometimes forming bridges/pendants and link cappings	None observed	
53–59	Cg	Sandstone	White (5Y 8/1)	None observed	None observed	

Category 4: pedotype 154 m above base of HCFm; 86.5 m above base of Horsethief Canyon section; 55–152 cm thick; mean thickness 104.4 cm

Mack et al.'s (1993) paleosol type: argillic gleysol with well-drained upper horizons

Depth (cm)	Horizon	Lithology	Color	B-fabric and Illuvial features	Redoximorphic features	Notes
0–26	A	Mudstone with dispersed organic matter	Dark olive gray (5Y 3/2)	Stipple speckled to mosaic speckled b-fabric Rare granostriation Uncommon, weakly developed clay coatings Rare iron hypocoatings around root traces Moderate iron impregnation with clouds of weak impregnation	None observed	Root traces Abundant bioturbation
26–49	Bw	Mudstone	Olive gray (5Y 4/2)	Stipple speckled to mosaic speckled b-fabric Uncommon, weakly developed clay coatings Large clouds of weak iron impregnation surrounded by rims of moderate impregnation	None observed	
49–74	Bg1	Mudstone	Black (5Y 2.5/1)	Mosaic speckled to unistriated b-fabric Common, weakly developed clay coatings	Common ferruginous redoximorphic features (masses)	Possible root traces Rare, 20 μm sphaerosiderite
74–99	Bg2	Mudstone	Olive gray (5Y 4/2)	Mosaic speckled b-fabric Common, weakly-developed clay coatings	Common ferruginous redoximorphic features (masses)	Common, 20–30 μm sphaerosiderite
99–136	Cg	Mudstone	Black (2.5Y 2.5/1)	Stipple-speckled to mosaic speckled b-fabric Rare granostriation Common, weakly-developed clay coatings	Rare ferruginous redoximorphic features (masses)	Uncommon, 5–10 μm sphaerosiderite

Category 5: pedotype 147 m above base of HCFm; 64 m above base of Horsethief Canyon section; 54–143 cm thick; mean thickness 98.5 cm

Mack et al.'s (1993) paleosol type: vertisol

Depth (cm)	Horizon	Lithology	Color	B-fabric and Illuvial features	Redoximorphic features	Notes
0–9	A	Mudstone	Dark grayish brown (10YR 4/2)	Mosaic speckled b-fabric Uncommon, weakly developed clay coatings Rare iron hypocoatings along root traces Weak to moderate iron impregnation in subparallel, linear zones	None observed	Root traces
9–18	ABss	Mudstone	Light brownish gray (2.5Y 6/2)	Stipple speckled to mosaic speckled b-fabric Uncommon granostriation Uncommon, weakly developed clay coatings Rare iron hypocoatings along root traces Clouds of weak to moderate iron impregnation	None observed	Root traces, Well-developed slickensides
18–30	Btss	Mudstone	Very dark grayish brown (2.5Y 3/2)	Stipple speckled to mosaic speckled b-fabric Rare, well-developed clay coatings Uncommon iron hypocoatings along root traces Weak iron impregnation with narrow, irregular zones of moderate impregnation	None observed	Root traces, Well-developed slickensides
30–54	Bw	Mudstone	Very dark grayish brown (2.5Y 3/2)	Mosaic speckled b-fabric Uncommon, moderately developed clay coatings Moderate iron impregnation in irregular, elongate zones separating clouds of weakly impregnated groundmass	None observed	

Category 6: pedotype 154 m above base of HCFm; 20 m above base of Morrin Bridge section; 53–177 cm thick; mean thickness 105.8 cm

Mack et al.'s (1993) paleosol type: argillisol

Depth (cm)	Horizon	Lithology	Color	B-fabric and Illuvial features	Redoximorphic features	Notes
0–21	Bt	Claystone	Olive gray (5Y 4/2)	Stipple speckled to mosaic speckled b-fabric Uncommon granostriation Common, moderately developed clay coatings Rare iron hypocoatings along voids/root traces Large clouds of weak iron impregnation with thick rims and clouds of moderate iron impregnation	None observed	Peds subangular, blocky
21–50	Bw1	Mudstone	Olive gray (5Y 4/2)	Mosaic speckled b-fabric Uncommon iron coatings on voids and along voids/root traces Weak to moderate iron impregnation	None observed	Uncommon sparry carbonate accumulation in voids and sparry to micritic matrix
50–60	Bw2	Mudstone	Dark olive gray (5Y 3/2)	Stipple-speckled to mosaic speckled b-fabric Uncommon, moderately developed clay coatings Large clouds of weak iron impregnation with thick rims and clouds of moderate iron impregnation, some surrounding root traces	None observed	Root traces
60–96	Bw3	Mudstone	Olive gray (5Y 4/2)	Stipple-speckled to weakly mosaic speckled b-fabric Uncommon, weakly developed clay coatings Large clouds of weak iron impregnation with moderate accumulation occurring in thick rims and small clouds	None observed	
96–124	Bw4	Sandy Mudstone	Olive gray (5Y 5/2)	Stipple-speckled to weakly mosaic speckled b-fabric Rare granostriation Rare clay coatings	Weak iron impregnation	None observed

(continued on next page)

Table 1 (*continued*)

Depth (cm)	Horizon	Lithology	Color	B-fabric and Illuvial features	Redoximorphic features	Notes
Category 7: pedotype 199 m above base of HCFm; 19 m above base of Tolman Bridge Section; 109–130 cm thick; mean thickness 116.3 cm						
Mack et al.'s (1993) paleosol type: argillic protosol						
0–62	Bw1	Sandy mudstone	Olive gray (5Y 5/2)	Stipple speckled to mosaic speckled b-fabric Uncommon, well-developed clay coatings Common iron coatings in voids and on grains Weak to strong iron impregnation	None observed	
62–130 (top of horizon)	Bw2	Sandy mudstone	Olive gray (5Y 5/2)	Stipple speckled to mosaic speckled b-fabric Uncommon, well-developed clay coatings Uncommon iron coatings in voids and on grains Large clouds of weak iron impregnation with rims of moderate	None observed	
Category 8: pedotype 56 m above base of HCFm; 10 m above base of Settling Ponds Section; 200 cm thick						
Mack et al.'s (1993) paleosol type: well-drained histosol or humic/melanic soil of Fey (2010)						
0–30	O	Coal	Black	None observed	None observed	
30–55	A	Siltstone	Light brownish gray (10YR 6/2)	Mosaic speckled to unistriated b-fabric Uncommon iron coatings on grains and hypocoatings along possible root traces Weak to moderate iron impregnation	None observed	Possible burrow, root traces
52–77	Bw1	Siltstone	Grayish brown (10YR 5/2)	Well-developed unistriated to faint reticulate b-fabric (slickensides) Granostriation Rare clay coatings Weak to moderate iron impregnation	None observed	Root traces
77–95	Bw2	Siltstone	Grayish brown (10YR 5/2)	Stipple-speckled to mosaic-speckled b-fabric Rare clay coatings Common granostriation Uncommon iron coatings on grains and hypocoatings along root traces and/or Weak to moderate iron impregnation	None observed	Burrow
95–130	Bw3	Mudstone	Light brownish gray (10YR 6/2)	Stipple-speckled b-fabric Weak to moderate iron impregnation	None observed	Root traces
130–200	Bw4	Siltstone	Light brownish	Very well developed mosaic-speckled b-fabric Rare clay coatings	None observed	Root traces

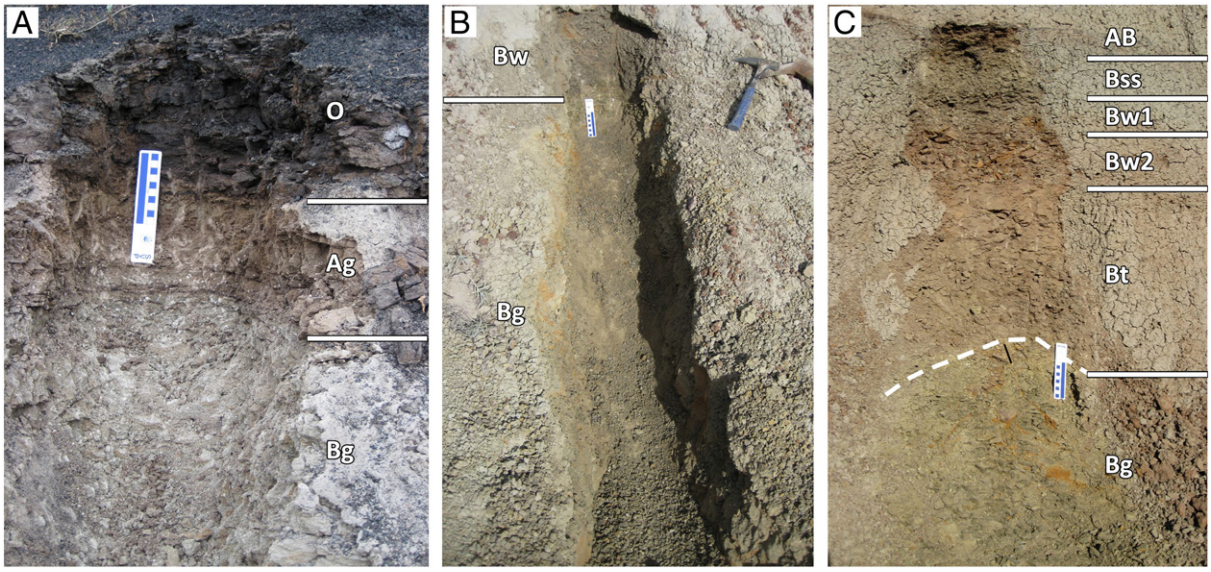

Fig. 5. Photographs of representative Horseshoe Canyon pedotypes. A) Hydromorphic paleosol (Category 1, Unit 1). B) Moderately-drained paleosol (Category 4, Unit 2). C) Well-drained paleosol (Category 5, Unit 2) displaying gleyed horizon at base of profile.

(Fig. 5C). Slickensides are well-developed and clay-coatings are common in higher-chroma horizons, but both of these pedogenic features are rare to absent in the basal gleyed horizon. Occasionally, tongues of the basal low-chroma horizon extend into the overlying horizon. Category 5 paleosols are moderately differentiated geochemically, exhibiting slight increases in the salinization, calcification, and clayeness ratios upward through the profile (Fig. 4). Similar to Category 4 paleosols, a lower leaching ratio than in Category 1–3 paleosols is observed.

4.6. Category 6 paleosols: higher-chroma green profiles with carbonate accumulation

This pedotype is uncommon in the HCFm, representing 5% of the paleosols (n = 4). Category 6 paleosols consist of higher-chroma, olive-green horizons that fine upwards from sandy mudstone to claystone (Fig. 4, Table 1). Evidence of bioturbation (in the form of elongate, small to large, branching root traces and sub-vertical burrows) is visible in these profiles and is especially prominent in the uppermost horizons. Iron coatings are present in most horizons. Microscopic carbonate accumulation is uncommon and occurs in specific horizons, either as sparry in-filling of voids (possibly root channels) or as small, micritic to predominantly sparry accumulation in the groundmass (Fig. 6E).

The geochemical profiles of Category 6 paleosols reveal compositional variation, indicating better horizon differentiation than in previous profiles. A slight increase in the leaching ratio is observed with increasing depth and the calcification ratio displays variation throughout the profile. No obvious correlation between the calcification ratio and the occurrence of pedogenic carbonate exists. Despite the similarly high calcification ratios in all analyzed profiles of this pedotype, carbonate accumulation is only observed in paleosol profiles from Unit 2 and not in those from Unit 1. As with Category 4 and 5 paleosols, higher calcification ratios and lower leaching ratios relative to Category 1–3 paleosols are observed (Fig. 4).

4.7. Category 7 paleosols: higher-chroma green profiles with weak horizon differentiation

This pedotype is uncommon in the HCFm, representing 4% of the paleosols (n = 3). Category 7 paleosols consist of bright, olive-green sandy mudstones that exhibit incipient horizon development (Fig. 4, Table 1). Clay coatings (Fig. 6F) and localized iron coatings are visible in thin sections and occur in all horizons. Additionally, traces of carbonate accumulation occur in the upper B horizon of one profile. Category 7 paleosols exhibit poor geochemical differentiation between horizons (Fig. 4). As in Category 4–6 paleosols, a higher calcification ratio and lower leaching ratio relative to Category 1–3 paleosols characterize Category 7 paleosols.

4.8. Category 8 paleosols: higher-chroma profiles capped by a thick, surficial coal horizon

This pedotype is rare in the HCFm, representing only 1% of the paleosols (n = 1). Category 8 paleosols consist of alternating, higher-chroma, brown and gray siltstone horizons capped by a 30 cm-thick coal horizon (Fig. 4, Table 1). Root traces occur throughout the profile, with the occurrence of burrows restricted to the upper portion of the profile. Clay accumulation, redoximorphic features (ferruginous masses), and slickensides are uncommon. Tendrils of the surficial horizon are observed extending into the underlying horizon. Category 8 paleosols are well differentiated geochemically (Fig. 4).

5. Discussion

5.1. Palaeoenvironmental interpretation of pedotypes

Pedogenic features and pedotypes reveal the presence of three soil drainage conditions within the HCFm: poorly-drained, well-drained, and transitional palaeoenvironments. Generally, all the paleosols of the HCFm exhibit relatively low-chroma colors (chroma ≤ 2) making interpretation of gley and poor drainage conditions based on color problematic. Consequently, pedogenic features such as redoximorphic features were utilized to aid our identification of hydromorphic horizons (i.e. Vepraskas, 1992).

5.1.1. Poorly-drained palaeoenvironments

The widespread occurrence of redoximorphic features, the presence of thick, organic-rich (A or O) surficial horizons and the weak geochemical differentiation of horizons in Category 1–3 paleosols indicate they are hydromorphic paleosols (gleyed histosols, gleysols, and gleyed protosols; see Table 1) that formed in environments with impeded drainage (e.g. Therrien et al., 2009). This interpretation is consistent with the gleyed color (chroma = 1) of these paleosols, which indicates that a high watertable saturated the entire soil profile

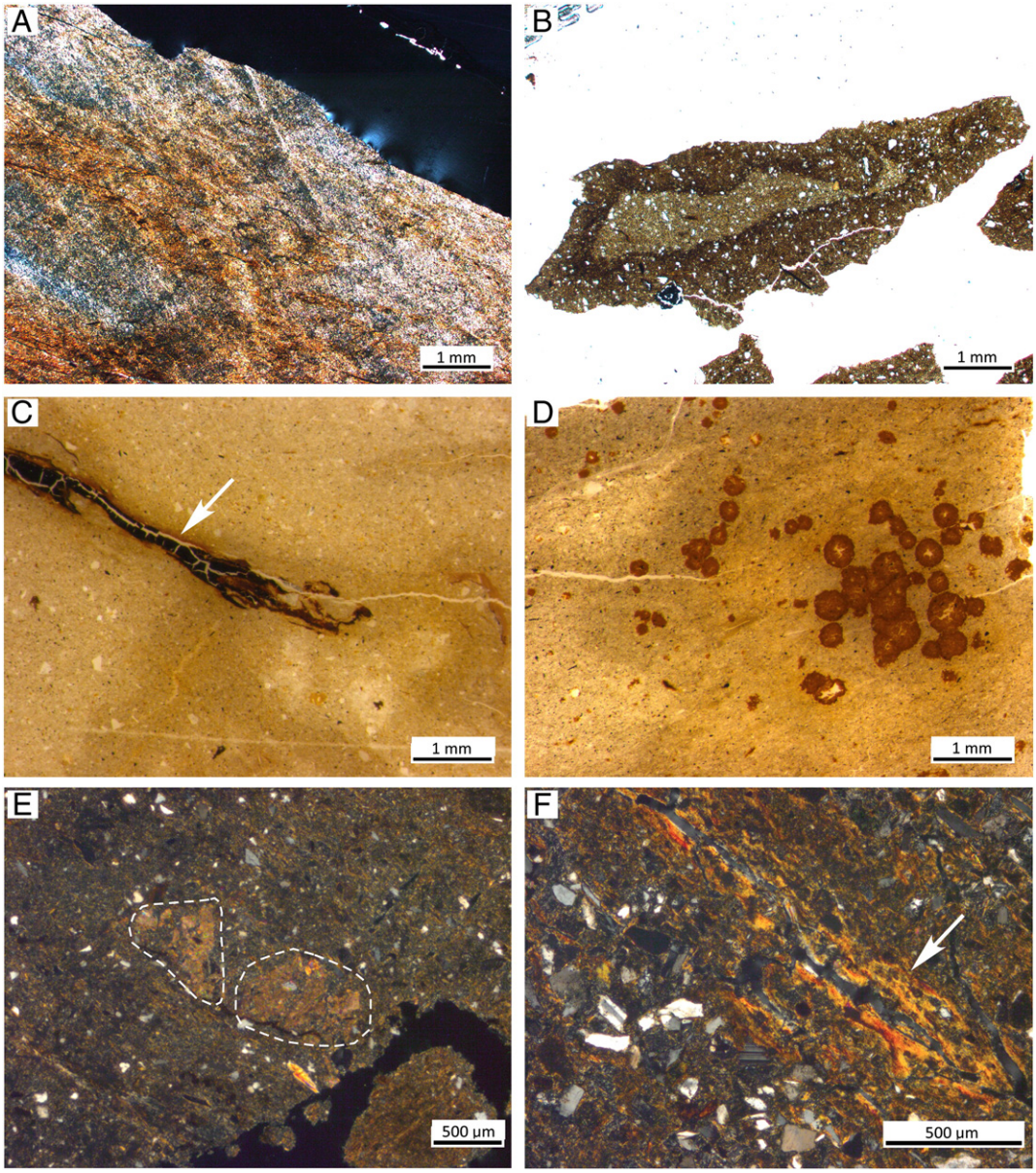

Fig. 6. Photomicrographs of pedogenic features observed in Horseshoe Canyon paleosols, in cross polarized (XPL) and plane polarized (PPL) light. A) Reticulate striated b-fabric formed by slickensides (XPL, Category 2). B) Redoximorphic feature with an iron-depleted center and iron-enriched rim (PPL, Category 2). C) Carbonaceous root fossil surrounded by iron hypocoating (arrow). Lighter areas surrounding root represent iron-depleted groundmass of gleyed horizon (PPL, Category 2). D) Sphaerosiderite nodules (PPL, Category 4). E) Microscopic carbonate accumulation in groundmass (XPL, Category 6). F) Clay coating along root trace (XPL, Category 7).

for 3–6 months per year (Daniels et al., 1971). The presence of carbonaceous root traces supports this interpretation (McCabe and Parrish, 1992; Kraus and Hasiotis, 2006). Although the watertable saturated the entire paleosol profile, the presence of slickensides and clay coatings indicates that free drainage occurred periodically (PiPujol and Buurman, 1994; Wright et al., 2000). Increases in the leaching weathering ratio at the top of some profiles also suggest that the uppermost horizons were subject to periods of free drainage (see Feakes and Retallack, 1988). Organic matter content of the parent material is believed to be responsible for differences in color among some of the profiles (e.g., Category 2a–c paleosols; see Dobos et al., 1990 and Sheldon, 2005). The greater abundance of clay coatings and redoximorphic features, combined with the unusually high leaching ratio, of Category 3 paleosols relative to other hydromorphic paleosols does not reflect changes in environmental conditions but probably the coarser nature of the parent material, which increases porosity and permeability (see Boggs, 2006).

5.1.2. Well-drained palaeoenvironments

The abundance of pedogenic features (i.e. clay coatings, iron coatings, and slickensides), the greater geochemical differentiation of horizons, and the prevalence of higher-chroma colors in Category 5–8 paleosols suggest that these paleosols formed in well-drained environments subject to alternating wet and dry conditions related to variable rainfall (vertisols, argillisols, argillic protosols, and well-drained histosols or humic/melanic paleosols; see Table 1). The co-occurrence of clay coatings with slickensides reveals periodic rainfall saturation followed by dry conditions (see Moeyersons et al., 2006; Nordt and Driese, 2009). The presence of ferruginous coatings and sparry carbonate accumulations in Category 6 paleosols also indicates that precipitation occasionally saturated these profiles. Sparry calcite accumulation is known to form as a result of short bursts of rainfall during the dry season (Drees and Wilding, 1987; Kraus and Hasiotis, 2006). The presence of a gleyed horizon at the base of a single profile (Fig. 5C) suggests that extended periods

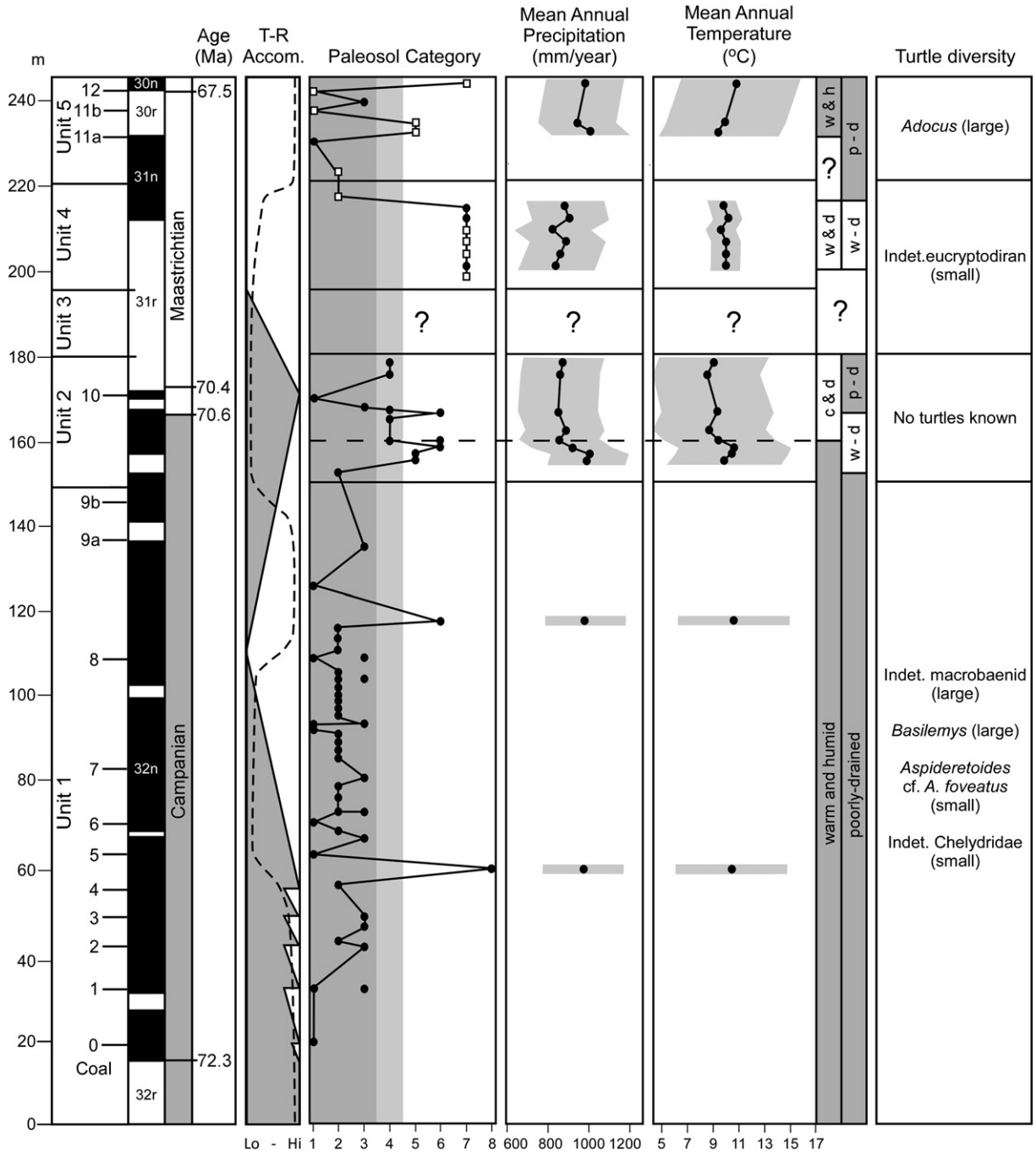

Fig. 7. Composite section showing stratigraphic distribution of paleosols, palaeoenvironmental indicators, and turtle faunal assemblages through the Horseshoe Canyon Formation. Paleosol categories are grouped into poorly-drained (dark gray), moderately-drained (light gray), and well-drained (white) palaeoenvironments. Gray boxes surrounding temperature and precipitation estimates illustrate error of estimate (from Sheldon and Tabor, 2009). Horizontal dash line marks beginning of cooling and aridification trend in Unit 2 prior to the Campanian–Maastrichtian boundary. Paleosols observed by Forkner (2002) are represented by white squares. Sea level (T–R, shaded area) and accommodation (Accom., dash line) curves are based on Eberth and Braman (2012). Radiometric ages (from Ogg et al., 2004 and Eberth and Deino, 2005) are superimposed on the HCFm magnetostratigraphy of Lerbekmo and Braman (2002, 2005). Abbreviations: c & d, cool and dry; w & d, warm and dry; w & h, warm and humid, w.-d., well-drained; p.-d., poorly-drained.

of impeded drainage related to a fluctuating watertable was a rare occurrence. A single profile exhibiting an organic-rich surficial horizon (Category 8) is interpreted as either a well-drained, organic-rich histosol or a humic/melanic paleosol. Such soils develop in environments with abundant and evenly distributed rainfall where the accumulation rate of organic matter exceeds its decomposition rate, which is inhibited by nutrient deficiency and soil acidity (Fey, 2010). Compared to Category 1–3 paleosols, the higher calcification ratio and lower leaching ratio observed in some of the well-drained paleosols are inferred to represent a more alkaline watertable (see Ashley and Driese, 2000) and/or drier conditions and less leaching, respectively.

5.1.3. Transitional palaeoenvironments

Category 4 paleosols preserve pedogenic features indicative of free drainage in the upper part of the profile and impeded drainage in the lower part of the profile (argillic gleysols; see Table 1), and exhibit significant differences in the degree of geochemical differentiation between upper and lower horizons, suggesting development in

Table 2
Distribution of pedotypes through the Horseshoe Canyon Formation and inferred palaeoenvironmental settings. Pedotypes documented in this study are compared to those observed by Forkner (2002) at Knudsen's Farm.

Unit	Pedotypes (this study)	Palaeoenvironments (this study)	Stratigraphic section	Pedotypes observed by Forkner (2002)	Palaeoenvironments (Forkner, 2002)
5	1, 3	Wetlands	Tolman Bridge (and Knudsen's Farm)	1, 2, 5, 7	Wetlands and well-drained habitats
4	7	Well-drained habitats	Tolman Bridge (and Knudsen's Farm)	2, 7	Well-drained habitats and rare wetlands
3	None observed	n/a	Morrin Bridge, Tolman Bridge	Not studied	n/a
2	1, 2, 3, 4, 5, 6	Wetlands, wetlands with low watertable, and well-drained habitats	Horsethief Canyon, Morrin Bridge	Not studied	n/a
1	1, 2, 3, 6, 8	Wetlands and rare well-drained habitats	East Coulee, Hoodoos, Settling Ponds, Ski Hill, Kirkpatrick, Horsethief Canyon	Not studied	n/a

transitional (i.e., moderately-drained) palaeoenvironments. In these paleosols, the presence of sphaerosiderite and gleyed horizons in the lower part of the profile indicates that the watertable was present for an extended period of time (Daniels et al., 1971; Driese et al., 2010). In contrast, the upper part of the profile is characterized by the presence of clay and iron coatings and higher-chroma colors, which are indicative of free drainage. Higher values of salinization, clayeness, and calcification ratios in the upper part of the profile relative to the geochemically undifferentiated lower part of the profile also suggest that the upper part of the profile was better drained. As such, Category 4 paleosols are inferred to have developed in slightly better-drained environments than hydromorphic paleosols (Categories 1–3) but more poorly-drained environments than Category 5–8 paleosols (see Wright et al., 2000). Furthermore, a higher calcification ratio in these paleosols than in hydromorphic paleosols is inferred to represent a more alkaline watertable (see Ashley and Driese, 2000) and/or drier conditions.

5.2. Palaeoenvironmental changes through the HCFm inferred from the stratigraphic distribution of pedotypes

The eight pedotypes represent a continuum of soil drainage conditions from waterlogged to freely-drained palaeoenvironments. When the distribution of pedotypes is considered in a stratigraphic context, paleosols reveal that a clear change in soil drainage conditions occurred through the HCFm (Fig. 7, Table 2):

Table 3
Estimates of MAP and MAT based on the geochemical composition of Category 4–8 paleosols. Asterisk indicates values calculated from equation for poorly-developed paleosols (Sheldon and Tabor, 2009). Cross indicates values calculated from equation for vertisols (Nordt and Driese, 2012).

Unit	Paleosol category investigated	Stratigraphic position from base of HCFm (m)	MAT (°C)	MAP (mm/year)
5	7	242	11.0	984
	5	222	9.9	944†
	5	220	9.4	1012†
4	7	217	9.9*	888
	7	215	10.7*	905
	7	208	9.6*	833
	7	202	10.0*	903
	7	201	10.0*	864
	7	200	10.0*	841
3	None observed	n/a	n/a	n/a
2	4	179	9.3	876
	4	177	8.7	865
	6	166	9.3	858
	4	162	8.8	886
	4	160	9.4	858
	6	158	10.7	915
	5	156	10.6	1018†
	5	155	9.9	991†
1	6	120	10.7	976
	8	60	10.5	968
Standard error of estimate:			4.4/0.6*	181/146†

1) Poorly-drained palaeoenvironments, characterized by a high but occasionally fluctuating watertable, prevailed in Unit 1. A well-drained paleosol occurring stratigraphically high in Unit 1 represents the onset of a change in drainage regime preceding the lithological change at the Unit 1/Unit 2 contact.
2) Poorly-drained palaeoenvironments persisted across the Unit 1/Unit 2 contact, but drainage subsequently improved through the lower portion of Unit 2. A brief return of poor drainage conditions at the level of Coal 10 coincided with the maximum transgression of the Drumheller Marine Tongue, but soil drainage subsequently improved above this marker bed.
3) The absence of paleosols in Unit 3 prevents documentation of the palaeoenvironmental conditions in this stratigraphic unit.
4) Well-drained palaeoenvironments prevailed in Unit 4. The occurrence of a hydromorphic paleosol at the top of Unit 4 reflects a change in soil drainage conditions and a rise in watertable level immediately prior to the Unit 4/Unit 5 contact. This paleosol represents the early onset of poorly-drained conditions prevalent in Unit 5 (see Section 5.4), demonstrating that the palaeoenvironmental changes preceded the Unit 4/Unit 5 transition and occurred gradually. An increase in organic-rich facies at the top of Unit 4 in Dry Island Buffalo Jump Provincial Park (Eberth and Currie, 2010), located ~10 km north of the study area, supports the timing of these palaeoenvironmental changes.
5) Drainage became impeded in Unit 5, producing poorly-drained palaeoenvironments characterized by a high but occasionally fluctuating watertable reminiscent of the conditions observed in Unit 1. The return of poorly-drained palaeoenvironments in Unit 5 has been attributed either to marine transgressions (Hamblin, 2004) or high accommodation (Eberth and Braman, 2012). The abundance of well-drained paleosols (unlike in Unit 1) and their occurrence between coal seams argue against a marine influence and suggest, instead, that paleosol hydrology reflects landscape changes associated with fluvial mechanisms (e.g., avulsion; Kraus and Aslan, 1993).

5.3. Palaeoclimatic reconstruction of the HCFm

The geochemical composition of well-drained and moderately-drained paleosols reveals that mean annual temperature (MAT) varied roughly between 9 °C and 11 °C and mean annual precipitation (MAP) fluctuated between 840 mm/year and 1020 mm/year during deposition of the HCFm (Table 3). When considered in a stratigraphic context, paleosols reveal clear evidence for palaeoclimatic changes through the formation (Fig. 7). The paucity of well-drained paleosols in Unit 1 greatly hinders palaeoclimatic reconstruction of this stratigraphic interval. Based on two well-drained paleosols, warm and humid conditions (mean MAT approximately 11 °C, mean MAP 964 mm/year) prevailed in the middle and upper part of Unit 1. These estimates are consistent with the climatic conditions under which modern examples of well-drained, organic-rich soils (Category 8) develop (Hoffman and Todd, 2000) and, within estimate error, those inferred based on palaeobotanical studies (Srivastava, 1970; Wolfe and Upchurch, 1987). Because no major palynological or lithological changes occur within Unit 1 (Eberth

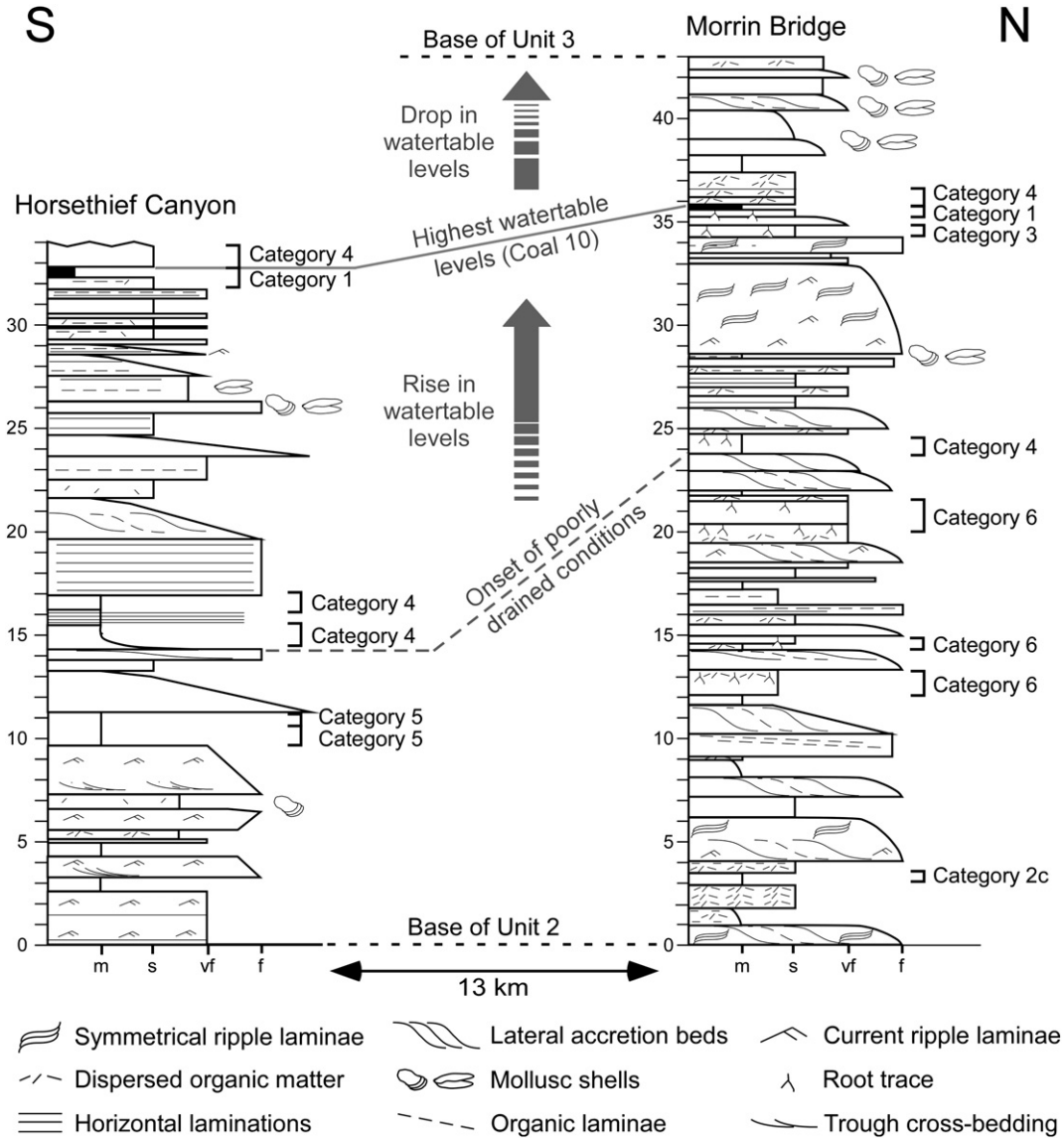

Fig. 8. Differential onset of poorly-drained conditions in Unit 2. Correlation between measured sections shows that poorly-drained conditions first occur stratigraphically lower at southern locations (Horsethief Canyon section) than at northern locations (Morrin Bridge section) due to the northward transgression of the Drumheller Marine Tongue.

and Braman, 2012) that could reflect climatic differences, we tentatively propose that this palaeoclimatic reconstruction is applicable to the entire unit.

Warm and humid conditions persisted across the Unit 1/Unit 2 boundary but climate changed higher in Unit 2, approximately 15 m above the base of the unit and 3.5 m below the Campanian–Maastrichtian boundary identified by Lerbekmo and Braman (2002). Within a short stratigraphic interval (~4 m), a cooling and aridification trend took place where MAT dropped by approximately 2 °C and MAP by 183 mm/year (Table 3). Cooler and drier conditions (mean MAT 9 °C and mean MAP 871 mm/year) persisted through the remainder of Unit 2.

The climate during deposition of Unit 4 was warmer (mean MAT approximately 10 °C) than in Unit 2 although precipitation levels remained low (mean MAP 874 mm//year). Unfortunately, the absence of paleosols in Unit 3 precludes determination of the rate at which the rise in temperature between Unit 2 and Unit 4 occurred. A gradual increase in precipitation is observed towards the Unit 4/Unit 5 contact and culminates with an increase in precipitation (>120 mm/year) across the lithological boundary but without concomitant increase in temperature. The warm and humid conditions that prevailed during deposition of Unit 5 (mean MAT approximately 10 °C, mean MAP 980 mm/year) indicate a return of climatic conditions previously observed in Unit 1.

These results reveal that a warm and humid climate prevailed during the latest Campanian. A rapid cooling and aridification trend occurred shortly prior to the Campanian–Maastrichtian boundary, resulting in a cool and dry climate during the earliest Maastrichtian. Mean annual temperatures returned to latest Campanian levels shortly thereafter whereas the increase in precipitation occurred over a longer time interval.

5.4. Influence of tectonism, base level, and climate on the development of HCFm paleosols

Lithological differences between the various stratigraphic units of the HCFm have often been inferred to represent, at least in part, changes in climatic regimes (e.g., Brinkman, 2003; Hamblin, 2004; Brinkman and Eberth, 2006; Eberth and Braman, 2012). The present study, however, demonstrates that lithological changes within the HCFm are unreliable climatic indicators. For example, the disappearance of coal beds at the Unit 1/Unit 2 contact occurred 15 m below the first evidence of climate change, which is not associated with

a change in lithology or pedology (Fig. 8). Rather, lithological changes through the HCFm presumably reflect the influence of tectonism and sea level changes (also see Eberth, 2004; Quinney, 2011; Eberth and Braman, 2012).

Evidence that sea level changes significantly affected soil drainage conditions can be found at various stratigraphic levels within the HCFm (Fig. 7). Proximity to the Bearpaw Sea in Unit 1 (Hamblin, 2004; Eberth and Braman, 2012) likely contributed to high watertable levels and the predominance of hydromorphic paleosols and coal beds. The transition to better-drained palaeoenvironments observed in Unit 2 is probably related to a lowering of the watertable in response, at least in part, to the regression of the Bearpaw Sea (Hamblin, 2004; Eberth and Braman, 2012). The subsequent return of hydromorphic paleosols high in Unit 2 coincides with the Drumheller Marine Tongue transgression (Fig. 7). Interestingly, the onset of poorly-drained conditions occurs stratigraphically lower in the southern part of the study area than in the north (Figs. 2, 3 and 8). Such differences in the timing of the change in drainage conditions is presumably related to the northward transgression of the Drumheller Marine Tongue (Hamblin, 2004), as more southern areas would have been affected by the marine transgression (e.g., rise in sea and watertable levels, occurrence of marine invertebrates) earlier than northern areas.

Influence of basinal changes in accommodation, sediment supply, and tectonism can be recognized in the HCFm stratigraphic architecture (for a review, see Eberth and Braman, 2012), so it is likely that such drivers also affected paleosol development. Changes in accommodation during deposition of Unit 1 do not appear to have influenced paleosol development (Fig. 7), possibly because high watertable levels related to the proximity of the shoreline overrode tectonic signals (see McCarthy et al., 1997). A decrease in accommodation at the base of Unit 2, in association with low sea levels, may have contributed to the development of well-drained conditions. Low accommodation conditions inferred for Units 3 and 4 should have resulted in the development of mature paleosols (Kraus, 1999), but Unit 4 consists predominantly of poorly-developed paleosols (Fig. 7). Although such paleosols could support the interpretation of a landscape subject to frequent reworking (Eberth and Braman, 2012), it is possible that their immaturity reflects development during the onset of basin subsidence (see Kraus, 2002). The return of hydromorphic paleosols near the top of Unit 4 and in Unit 5 coincides with an increase in accommodation, as well as in precipitation and temperature (Fig. 7). Autocyclic fluvial events (i.e. channel migration) are presumably responsible for the development of well-drained paleosols in Unit 5 (Kraus and Aslan, 1999; Forkner, 2002).

Our results underscore the fact that lithological changes can be poor climatic indicators, as numerous other factors can lead to lithological and pedological differences (e.g., Kraus, 1999; Retallack, 2001; Sheldon and Tabor, 2009). Furthermore, paleosols from the HCFm demonstrate that climatic changes do not always correspond with discernible changes in lithologies or pedotypes but can only be identified based on the geochemical composition of paleosols. Consequently, terrestrial palaeoenvironmental reconstructions should involve detailed palaeopedological investigations and not simply rely on lithological changes within a formation.

5.5. Fossil turtle turnover and palaeoenvironmental changes in the HCFm

A dramatic fossil turtle turnover has been recognized within the HCFm (Brinkman, 2003; Brinkman and Eberth, 2006) whereby diversity and taxonomic composition of turtle assemblages vary significantly through the formation (Fig. 7): 1) four turtles are found in Unit 1, representing small (<30 cm carapace length) and large (>30 cm carapace length) species; 2) turtles are absent in Unit 2; 3) one rare, very small (<10 cm carapace length; D.B. Brinkman, pers. comm. 2012) turtle is found in Units 3 and 4; and 4) at least one large turtle occurs in Unit 5. Because the turnover in turtle fauna appears to coincide with climatic changes inferred from leaf physiognomy, the decline in turtle diversity in the middle of the HCFm was hypothesized to be related to a climatic cooling event (Brinkman, 2003; Brinkman and Eberth, 2006).

Comparison of the stratigraphic distribution of fossil turtles with that of pedogenic palaeoenvironmental indicators refines the proposed scenario for the turtle turnover within the HCFm (Fig. 7). Results reveal that the disappearance of turtles at the Unit 1/Unit 2 contact precedes the decline in palaeotemperature and palaeoprecipitation observed in Unit 2 but corresponds closely to the transition from poorly-drained to well-drained palaeoenvironments. In turn, the low turtle diversity in Unit 4 coincides with warm annual temperatures, similar to those recorded in Unit 1, but lower annual precipitation and the absence of wetlands. Finally although the low diversity and scarcity of turtle remains in Unit 5 could be an underrepresentation due to fossil preservation biases (see Brinkman and Eberth, 2006), the presence of a large taxon in this unit coincides with the return of a warm and humid climate and poorly-drained palaeoenvironments similar to those observed in Unit 1. Thus, our results reveal that the decline in turtle diversity in the HCFm did not coincide with cooler climatic conditions but must be related to other factors. Similarly, changes in turtle diversity through the lower Eocene Willwood Formation have been shown to not coincide with climatic conditions and were hypothesized to correspond to changes in habitat heterogeneity instead (Holroyd and Hutchison, 2001).

The fact that the greatest diversity and largest species of turtles occur in poorly-drained palaeoenvironments suggests that turtle diversity in the HCFm is primarily controlled by soil drainage conditions. Among extant turtles, species richness is correlated with driest month rainfall and total annual rainfall (Iverson, 1992) as well as with various wetland characteristics, such as low annual duration of dry conditions, frequency of flooding, connectedness of scours, and water turbidity (Bodie et al., 2000). It is thus likely that the disappearance of various wetlands, rather than climate change, is responsible for the decline in turtle diversity through the HCFm. Other factors, such as aridity, landscape instability, or barriers restricting the migration of new taxa in the area, may also have restricted turtle diversity recovery (e.g., in Unit 4 and/or 5), but further work is required to determine the importance of these factors.

6. Conclusions

Palaeopedological and geochemical analyses confirm that important climatic changes occurred during deposition of the late Campanian–early Maastrichtian Horseshoe Canyon Formation, but these climatic changes do not coincide with intraformational lithological changes as previously inferred. Changes in soil drainage conditions generally coincide with formational subdivisions established based on lithological differences, but climatic changes occur within subdivisions without concomitant lithological or pedological changes. Tectonism and sea level changes appear to have had a significant influence on watertable levels and paleosol development. Warm and humid conditions (MAT ~10 °C, MAP ~1000 mm/year) prevailed during deposition of the HCFm and were only interrupted by a rapid decrease in temperature and precipitation (MAT ~9 °C, MAP ~870 mm/year) just before the Campanian–Maastrichtian boundary. Contrary to previously hypothesized, the timing of this cool and dry interval does not coincide with documented changes in HCFm turtle assemblages. Rather, the fossil turtle turnover appears to follow closely changes in soil drainage conditions, with aridity and migratory barriers acting as possible limiting factors to turtle fauna recovery.

Acknowledgments

We thank Dennis Braman and Don Brinkman for their helpful discussions and willingness to share information during the course of

this project. We also thank Amanda McGee, Jeff Quinney, Kohei Tanaka and Malcolm Williamson for their assistance in the field. Constructive comments by Nathan Sheldon, an anonymous reviewer, and editor Finn Surlyk greatly improved this manuscript. The project was funded by a Natural Sciences and Engineering Research Council (NSERC) Master's scholarship (AQ), a NSERC Discovery grant (DKZ) as well as grants from the Royal Tyrrell Museum Cooperating Society (AQ and FT) and the Dinosaur Research Institute (AQ). This research was conducted as part of A. Quinney's Master thesis at the University of Calgary in the Department of Geoscience.

References

Ashley, G.M., Driese, S.G., 2000. Paleopedology and paleohydrology of a volcaniclastic paleosol interval: implications for early Pleistocene stratigraphy and paleoclimate record, Olduvai Gorge, Tanzania. Journal of Sedimentary Research 70, 1065–1080.

Bodie, J.R., Semlitsch, R.D., Renken, R.B., 2000. Diversity and structure of turtle assemblages: associations with wetland characters across a floodplain landscape. Ecography 23, 444–456.

Boggs, S., 2006. Principles of Sedimentology and Stratigraphy, 4th edition. Pearson Prentice Hall, Upper Saddle River, New Jersey.

Brinkman, D.B., 2003. A review of nonmarine turtles from the Late Cretaceous of Alberta. Canadian Journal of Earth Sciences 40, 557–571.

Brinkman, D.B., Eberth, D.A., 2006. Turtles of the Horseshoe Canyon and Scollard formations: further evidence fo a biotic response to Late Cretaceous climate change. Fossil Turtle Research 1, 11–18.

Bullock, P., Federoff, N., Jongerius, A., Stoops, G., Tursina, T., 1985. Handbook for Soil Thin Section Description. Waine Research Publications, Albrighton, England.

Cant, D., Stockmal, G., 1989. The Alberta foreland basin: relationship between stratigraphy and Cordilleran terrane-accretion events. Canadian Journal of Earth Sciences 26, 1964–1975.

Catuneanu, O., Sweet, A.R., Miall, A.D., 2000. Reciprocal stratigraphy of the Campanian–Paleocene Western Interior of North America. Sedimentary Geology 134, 235–255.

Chadwick, O.A., Brimhall, G.H., Hendricks, D.M., 1990. From a black to a gray box: a mass balance interpretation of pedogenesis. Geomorphology 3, 369–390.

Dahms, D.E., 1998. Soil taxonomy and paleoenvironmental reconstruction: a critical commentary. Quaternary International 51 (52), 58–60.

Dahms, D.E., Holiday, V.T., 1998. Soil taxonomy and paleoenvironmental reconstruction: a critical review. Quaternary International 51 (52), 109–114.

Daniels, R.B., Gamble, E.E., Nelson, L.A., 1971. Relations between soil morphology and water-table levels on a dissected North Carolina coastal plain. Soil Science Society of America Journal 35, 781–784.

Dobos, R.R., Ciolkosz, E.J., Waltman, W.J., 1990. The effect of organic carbon, temperature, time, and redox conditions on soil color. Soil Science 150, 506–512.

Drees, L.R., Wilding, L.P., 1987. Micromorphic record and interpretations of carbonate forms in the rolling plains of Texas. Geoderma 40, 157–175.

Driese, S.G., Mora, C.I., Stiles, C.A., Joeckel, R.M., Nordt, L.C., 2000. Mass-balance reconstruction of a modern Vertisol: implications for interpreting the geochemistry and burial alteration of paleo-Vertisols. Geoderma 95, 179–204.

Driese, S.G., Ludvigson, G.A., Roberts, J.A., Fowle, D.A., Gonzalez, L.A., Smith, J.J., Vulava, V.M., McKay, L.D., 2010. Micromorphology and stable-isotope geochemistry of historical pedogenic siderite formed in PAH-contaminated alluvial clay soils, Tennessee, U.S.A. Journal of Sedimentary Research 80, 943–954.

Eberth, D.A., 2004. A revised stratigraphy for the Edmonton Group (Upper Cretaceous) and its potential sandstone reservoirs. ICE 2004 field trip No. 7 guidebook, CSPG-CHOA-CWLS Joint Conference, Calgary, Alberta, pp. 1–45.

Eberth, D.A., Braman, D.R., 2012. A revised stratigraphy and depositional history for the Horseshoe Canyon Formation (Upper Cretaceous), southern Alberta plains. Canadian Journal of Earth Sciences 49, 1053–1083.

Eberth, D.A., Currie, P., 2010. Stratigraphy, sedimentology, and taphonomy of the *Albertosaurus* bonebed (upper Horseshoe Canyon Formation, Maastrichtian), southern Alberta, Canada. Canadian Journal of Earth Sciences 47, 1119–1143.

Eberth, D.A., Deino, A., 2005. New $^{40}Ar/^{39}Ar$ ages from three bentonites in the Bearpaw, Horseshoe Canyon and Scollard formations (Upper Cretaceous–Paleocene) of southern Alberta, Canada. In: Braman, D.R., Therrien, F., Koppelhus, E.B., Taylor, W. (Eds.), Dinosaur Park Symposium, Short Papers, Abstract, and Program, Royal Tyrrell Museum, Drumheller, Alberta. Special Publication of the Royal Tyrrell Museum, pp. 23–24.

Eberth, D.A., Currie, P.J., Brinkman, D.B., Ryan, M.J., Braman, D.R., Gardner, J.D., Lam, V.D., Spivak, D.N., Newman, A.G., 2001. Alberta's dinosaurs and other fossil vertebrates: Judith River and Edmonton groups (Campanian–Maastrichtian). In: Hills, C.L. (Ed.), Mesozoic and Cenozoic Paleontology in the Western Plains and Rocky Mountains: Guidebook for the Field Trips, Society of Vertebrate Paleontology, 61st Annual Meeting: Museum of the Rockies Occasional Paper No.3, pp. 49–75 (Bozeman, Montana).

Fastovsky, D.E., McSweeney, K., 1987. Paleosols spanning the Cretaceous–Paleogene transition, eastern Montana and western North Dakota. Geological Society of America Bulletin 99, 66–77.

Feakes, C.R., Retallack, G., 1988. Recognition and chemical characterization of fossil soils developed on alluvium: a Late Ordovician example. In: Reinhardt, J., Sigleo, W.R. (Eds.), Paleosols and Weathering Through Geologic Time: Principles and Applications. Geological Society of America Special Paper, Boulder, Colorado, pp. 35–48.

Fey, M., 2010. Soils of South Africa. Cambridge University Press, Cambridge.

Forkner, R.M., 2002. Paleoenvironmental variability across the Cretaceous–Tertiary boundary in the Alberta Foreland Basin, as interpreted from fluvial deposits and paleosols, Red Deer River Valley, Alberta, Canada, Unpublished M.Sc. thesis, Baylor University, Waco, Texas, 121 pp.

Gibson, D.W., 1977. Upper Cretaceous and Tertiary Coal-Bearing Strata in the Drumheller-Ardley Region, Red Deer River Valley, Alberta. Geological Survey of Canada Paper 76–35, 1–41.

Hamblin, A.P., 2004. The Horseshoe Canyon Formation in southern Alberta: surface and subsurface stratigraphic architecture, sedimentology, and resource potential. Geological Survey of Canada Bulletin 578, 1–180.

Hoffman, T., Todd, S., 2000. A national review of land degredation in South Africa: the influence of biophysical and socioeconomic factors. Journal of Southern African Studies 26, 17–36.

Holroyd, P.A., Hutchison, J.H., 2001. Turtle diversity and abundance through the lower Eocene Willwood Formation of the southern Bighorn Basin. In: Gingerich, P.D. (Ed.), Paleocene–Eocene Stratigraphy and Biotic Changes in the Bighorn and Clarks Fork Basins, Wyoming: University of Michigan Papers on Paleontology 33, pp. 97–107.

Irish, E.J.W., 1970. The Edmonton Group of south-central Alberta. Bulletin of Canadian Petroleum Geology 18, 125–155.

Iverson, J.B., 1992. Global correlates of species richness in turtles. Journal of Herpetology 3, 77–81.

Khidir, A., Catuneanu, O., 2009. Basin-scale distribution of authigenic clay minerals in the late Maastrichtian–early Paleocene fluvial strata of the Alberta foredeep: implications for burial depth. Bulletin of Canadian Petroleum Geology 57, 251–274.

Kraus, M.J., 1999. Paleosols in clastic sedimentary rocks: their geologic applications. Earth-Science Reviews 47, 387–406.

Kraus, M.J., 2002. Basin-scale changes in floodplain paleosols: implications for interpreting alluvial architecture. Journal of Sedimentary Research 72, 500–509.

Kraus, M.J., Aslan, A., 1993. Eocene hydromorphic paleosols: significance for interpreting ancient floodplain processes. Journal of Sedimentary Petrology 63, 453–463.

Kraus, M.J., Aslan, A., 1999. Paleosol sequences in floodplain environments: a hierarchical approach. In: Thiry, M. (Editor), Palaeoweathering, Palaeosurfaces and Related Continental Deposits: International Association of Sedimentologists Special Publication, 27, pp. 303–321.

Kraus, M.J., Brown, T.M., 1986. Paleosols and time resolution in alluvial stratigraphy. In: Wright, P.V. (Ed.), Paleosols: Their Recognition and Interpretation. Princeton University Press, Princeton, N.J., pp. 180–207.

Kraus, M.J., Hasiotis, S.T., 2006. Significance of different modes of rhizolith preservation to interpreting paleoenvironmental and paleohydrologic settings: examples from Paleogene paleosols, Bighorn Basin, Wyoming, U.S.A. Journal of Sedimentary Research 76, 633–646.

Larson, D.W., Brinkman, D.B., Bell, P.R., 2010. Faunal assemblages from the upper Horseshoe Canyon Formation, an early Maastrichtian cool-climate assemblage from Alberta, with special reference to the *Albertosaurus sarcophagus* bonebed. Canadian Journal of Earth Sciences 47, 1159–1181.

Leckie, D.A., Smith, D.G., 1992. Regional setting, evolution, and depositional cycles of the Western Canada Sedimentary Basin. In: Macqueen, R.W., Leckie, D.A. (Eds.), Foreland Basins and Fold Belts: AAPG Memoir, 55, pp. 9–46.

Lerbekmo, J.F., Braman, D.R., 2002. Magnetostratigraphic and biostratigraphic correlation of late Campanian and Maastrichtian marine and continental strata from the Red Deer Valley to the Cypress Hills, Alberta, Canada. Canadian Journal of Earth Sciences 39, 539–557.

Lerbekmo, J.F., Braman, D.R., 2005. Magnetostratigraphic and palynostratigraphic correlation of the late Campanian to early Maastrichtian strata of the Bearpaw and Horseshoe Canyon formations between CPOG Strathmore corehole and the Red Deer Valley section, Alberta, Canada. Bulletin of Canadian Petroleum Geology 53, 154–164.

Mack, G.H., James, C.W., Monger, C., 1993. Classification of Paleosols. Geological Society of America Bulletin 105, 129–136.

Mallon, J.C., Holmes, R., Eberth, D.A., Ryan, M.J., Anderson, J.S., 2011. Variation in the skull of *Anchiceratops* (Dinosauria, Ceratopsidae) from the Horseshoe Canyon Formation (Upper Cretaceous) of Alberta. Journal of Vertebrate Paleontology 31, 1047–1071.

McCabe, P.J., Parrish, J.T., 1992. Tectonic and climatic controls on Cretaceous coals. In: McCabe, P.J., Parrish, J.T. (Eds.), Controls on the Distribution and Quality of Cretaceous Coals. Geological Society of America Special Paper 267, pp. 1–15.

McCabe, P.J., Strobl, R.S., Macdonald, D.E., Nurkowski, J., Bosman, A., 1989. Coal Resource Evaluation of the Horseshoe Canyon Formation and Laterally Equivalent Strata, to a Depth of 400 m, in the Alberta Plain Area. Alberta Research Council Open File Report 1989–7, 1–87.

McCarthy, P.J., Martini, P.I., Leckie, D.A., 1997. Anatomy and evolution of a Lower Cretaceous alluvial plain: sedimentology and palaeosols in the upper Blairmore Group, south-western Alberta, Canada. Sedimentology 44, 197–220.

Moeyersons, J., Nyssen, J., Poesen, J., Deckers, J., Haile, M., 2006. On the origin of rock fragment mulches on Vertisols: a case study from the Ethiopian highlands. Geomorphology 76, 411–429.

Munsell, 2005. Munsell Soil Colour Charts: Matte Collection. Macbeth Division of Kollmorgen Corp., Baltimore.

Nordt, L.C., Driese, S.G., 2009. Hydropedological model of vertisol formation along the Gulf Coast Prarie land resource area of Texas. Hydrology and Earth System Sciences 13, 2039–2053.

Nordt, L.C., Driese, S.G., 2012. New weathering index improves paleorainfall estimates from vertisols. Geology 38, 407–410.

Nurkowski, J., 1984. Coal quality, coal rank variation and its relation to reconstructed overburden, Upper Cretaceous and Tertiary plains coals, Alberta, Canada. American Association of Petroleum Geologists Bulletin 68, 285–295.

Ogg, J.G., Agterberg, F.P., Gradstein, F.M., 2004. The Cretaceous period. In: Gradstein, F.M., Ogg, J.G., Smith, A. (Eds.), A Geologic Time Scale. Cambridge University Press, Cambridge, pp. 344–383.
PiPujol, M.D., Buurman, P., 1994. The distinction between ground-water gley and surface-water gley phenomena in Tertiary paleosols of the Ebro Basin, NE Spain. Palaeogeography, Palaeoclimatology, Palaeoecology 110, 103–113.
Quinney, A., 2011. The Upper Cretaceous Horseshoe Canyon Formation: using paleosols to reconstruct ancient environments, climates, and record of climate change in a dinosaur-dominated terrestrial ecosystem, Unpublished M.Sc. thesis, University of Calgary, Calgary, Alberta, 145 pp.
Retallack, G., 1994. A pedotype approach to latest Cretaceous and earliest Tertiary paleosols in eastern Montana. Geological Society of America Bulletin 106, 1377–1397.
Retallack, G., 1997. A Colour Guide to Paleosols. John Wiley and Sons, New York.
Retallack, G., 2001. Soils of the Past: An Introduction to Paleopedology. Blackwell Science, Oxford.
Sheldon, N.D., 2005. Do red beds indicate paleoclimate?: A Permian case study. Palaeogeography, Palaeoclimatology, Palaeoecology 228, 305–319.
Sheldon, N.D., 2006. Quaternary Glacial–Interglacial cycles in Hawaii. Journal of Geology 114, 367–376.
Sheldon, N.D., Tabor, N.J., 2009. Quantitative paleoenvironmental and paleoclimatic reconstruction using paleosols. Earth-Science Reviews 95, 1–52.
Sheldon, N.D., Retallack, G., Tanaka, S., 2002. Geochemical climofunctions from North American soils and application to paleosols across the Eocene–Oligocene boundary in Oregon. Journal of Geology 110, 687–696.
Smith, A.G., Hurley, A.M., Briden, J.C., 1981. Phanerozoic Paleocontinental Maps. Cambridge University Press, Melbourne, Australia.
Srivastava, S.K., 1970. Pollen biostratigraphy and paleoecology of the Edmonton Formation (Maastrichtian), Alberta, Canada. Palaeogeography, Palaeoclimatology, Palaeoecology 7, 221–276.
Stott, D.F., 1984. Cretaceous sequences of the foothills of the Canadian Rocky Mountains. Canadian Society of Petroleum Geologists Memoir 9, 85–107.
Straight, W.H., Eberth, D.A., 2002. Testing the utility of vertebrate remains in recognizing patterns in fluvial deposits: an example from the lower Horseshoe Canyon Formation, Alberta. Palaios 17, 472–490.
Therrien, F., Zelenitsky, D.K., Weishampel, D.B., 2009. Palaeoenvironmental reconstruction of the Late Cretaceous Sânpetru Formation (Haţeg Basin, Romania) using paleosols and implications for the "disappearance" of dinosaurs. Palaeogeography, Palaeoclimatology, Palaeoecology 272, 37–52.
Vepraskas, M.J., 1992. Redoximorphic features for identifying aquic conditions. North Carolina Agricultural Research Services Technical Bulletin 301, 1–33.
Wolfe, J.A., Upchurch, G.R., 1987. North American nonmarine climates and vegetation during the Late Cretaceous. Palaeogeography, Palaeoclimatology, Palaeoecology 61, 33–77.
Wright, P.V., Taylor, K.G., Beck, V.H., 2000. The paleohydrology of Lower Cretaceous seasonal wetlands, Isle of Wight, southern England. Journal of Sedimentary Research 70, 619–632.
Wu, X., Brinkman, D.B., Eberth, D.A., Braman, D.R., 2007. A new ceratopsid dinosaur (Ornithischia) from the uppermost Horseshoe Canyon Formation (upper Maastrichtian), Alberta, Canada. Canadian Journal of Earth Sciences 44, 1243–1265.